



Collective phase transitions in confined fish schools

Chenchen Huang^a, Feng Ling^a, and Eva Kanso^{a,b,1}

Edited by David Weitz, Harvard University, Cambridge, MA; received March 27, 2024; accepted August 21, 2024

The collective patterns that emerge in schooling fish are often analyzed using models of self-propelled particles in unbounded domains. However, while schooling fish in both field and laboratory settings interact with domain boundaries, these effects are typically ignored. Here, we propose a model that incorporates geometric confinement, by accounting for both flow and wall interactions, into existing datadriven behavioral rules. We show that new collective phases emerge where the school of fish "follows the tank wall" or "double mills." Importantly, confinement induces repeated switching between two collective states, schooling and milling. We describe the group dynamics probabilistically, uncovering bistable collective states along with unintuitive bifurcations driving phase transitions. Our findings support the hypothesis that collective transitions in fish schools could occur spontaneously, with no adjustment at the individual level, and opens venues to control and engineer emergent collective patterns in biological and synthetic systems that operate far from equilibrium.

intermittency | coarse-grained dynamics | collective behavior | fish schools | confinement

Patterns in biology are dynamic. Biological systems at all length and time scales from chromosome segregation during cell division (1) and tissue remodeling during morphogenesis and cell renewal (2) to animal groups on the move (3, 4)—exhibit dynamic collective patterns that are intertwined with, and integral to, biological function. Fish schooling, a widespread phenomenon across species and marine habitats with ecological and ethological relevance (5), serves as a model system for studying self-organization and collective intelligence in social animals, in the absence of obvious leaders (3, 6, 7). The variety of the spatial patterns exhibited by fish schools are thought to confer functional advantages to the group's ability to migrate, forage, and respond to threats (8, 9) and are likely to have shaped the selection pressures experienced by individuals living in groups (10, 11).

Although schooling fish in the field and in laboratory settings interact with boundaries, most models ignore boundary effects. Phenomenological models of self-propelled particles following simple rules of avoidance, alignment, and attraction in unbounded domains were able to reproduce many of the collective patterns observed in fish schools, including disordered swarming, rotational milling, and polarized schooling (6, 12, 13). These early models were pivotal to the field of active matter physics because of their simplicity (14), universality (15), and suitability for continuum formulation (16, 17), but lacked a quantitative connection to biological observations. Later models inferred individual behavior directly from empirical data of fish in shallow water tanks (18, 19). However, although based on data collected under confinement, the collective behavior emerging from these models was analyzed in unbounded domains (20, 21). These studies reported, in addition to swarming, milling, and schooling, new global patterns. In ref. 20, an elongated milling pattern and dynamic transitions between milling and schooling were reported in very narrow ranges of alignment and attraction parameters. Transitions between schooling and milling also appeared in the simpler particle model (6) but under rare injections of large rotational noise (22, SI Appendix, Fig. 7). In ref. 21, far-field flow interactions were incorporated into the data-inferred models (18), leading to a novel collective turning pattern, but no spontaneous phase transitions.

Environmental factors, such as geometric confinement (9) and light intensity (23), affect the collective patterns obtained in experiments of schooling fish, giving rise to back-and-forth transitions between milling and polarized schooling (9, 23). However, the mechanisms that trigger these transitions are unclear. Do individual fish adjust their response with confinement (9) or with changes in illumination levels (23), thereby inducing collective transitions? Or do collective transitions emerge at the group level, without necessary adjustments at the individual level? Distinguishing between these two hypotheses is challenging experimentally. Mathematical models provide a powerful tool to probe these hypotheses. However, studies in unbounded domains (6, 9, 20-22)—even those where schooling-to-milling transitions emerged at curated choices of

Significance

Animal groups, bird flocks, fish schools, and even humans in a crowd, often move in cohesion, without an obvious leader, but how do they transition dynamically between collective states and how do environmental factors, such as confinement, affect these transitions? Here, we model schools of fish confined in circular tanks as self-propelled particles following behavioral rules and interacting with flows and geometric boundaries. We uncover collective patterns unseen in unbounded domains and surprising bistable collective states. Our findings explain empirical observations and open venues to engineer emergent collective patterns in biological and synthetic systems.

Author affiliations: ^aDepartment of Aerospace and Mechanical Engineering, University of Southern California, Los Angeles, CA 90089; and ^bDepartment of Physics and Astronomy, University of Southern California, Los Angeles, CA 90089

Author contributions: E.K. designed research; C.H. and E.K. performed research; C.H. and E.K. analyzed data; F.L. contributed to code development; and E.K. wrote the

The authors declare no competing interest.

This article is a PNAS Direct Submission.

Copyright © 2024 the Author(s), Published by PNAS. This article is distributed under Creative Commons Attribution-NonCommercial-NoDerivatives License 4.0

¹To whom correspondence may be addressed. Email:

This article contains supporting information online at https://www.pnas.org/lookup/suppl/doi:10.1073/pnas. 2406293121/-/DCSupplemental.

Published October 21, 2024.

parameters (20, 22)—are inherently unable, by model design, to examine the effects of interactions with boundaries (9). To date, and with an abundance of particle-based models describing the collective behavior of fish schools, we lack a rigorous framework for analyzing their emergent dynamics under confinement.

In this work, we establish a mathematical model of schooling fish that incorporates boundaries into data-inferred rules of self-propelled swimmers (18) and flow interactions (21). We demonstrate that geometric confinement triggers surprising changes in the collective patterns of the group, including the emergence of new phases unseen in unbounded domains and back-and-forth switching between schooling and milling. While the mechanisms driving these transitions are novel, we leverage previously proposed tools for analyzing intermittent behavior in one-dimensional schools of fish (22). Particularly, following refs. 22 and 24, we use a probabilistic data-driven approach to model the group dynamics using a Fokker-Planck equation, thus mapping the time evolution of individual-level variables to the time evolution of group-level variables. We construct effective potential landscapes at the collective level. This formulation allows us to distinguish between collective transitions that occur when changing individual-level parameters and transitions that arise from the existence of multiple metastable states at the group level.

Results

Mathematical Modeling. We modeled individual fish as selfpropelled particles moving in a planar circularly confined domain at a constant speed U (units $m \cdot s^{-1}$) relative to the flow. Each swimmer followed behavioral rules derived empirically from shallow-water experiments in a circular tank (18), where it gets attracted to its Voronoi neighbors with intensity k_p (m⁻¹·s⁻¹), aligns with the same neighbors with intensity k_v (m⁻¹), reorients to avoid collision with the tank wall with intensity k_w (m·s⁻¹), and is subject to a rotational white noise of SD σ (rad·s^{-1/2}).

Additionally, each swimmer is passively influenced by the far-field flow created by all other swimmers (21, 25). The farfield flow of an individual is approximated by a dipolar field of intensity $k_f = UA$ (units m³·s⁻¹) that depends on the swimmer's speed U and surface area $A = \pi \ell^2/4$, where ℓ is the body length of a typical swimmer (26-28). Except for estimating this flow disturbance, we considered all swimmers as pointlike particles. In circular confinement, to ensure no flux at the circular boundary, we introduced a system of image dipoles based on the Milne-Thomson circle theorem (28, 29).

Following ref. 21, we used U and k_p to define the characteristic length $U^{1/2}k_p^{-1/2}$ and time $(Uk_p)^{-1/2}$ scales and arrived at nondimensional counterparts of the alignment intensity $I_a=$ $k_v U^{1/2} k_p^{-1/2}$, noise intensity $I_n = \sigma(Uk_p)^{-1/4}$, intensity of wall-induced reorientation $I_w = k_w U^{-1}$, and dipole strength $I_f = k_f k_p U^{-2}$. The dimensionless tank radius is denoted by R. In nondimensional form, the motion of swimmer j, where j = $1, \ldots, N$ and N is the school size, follows the set of stochastic differential equations (SI Appendix, sections S.1–S.3 and Fig. S.1),

$$\dot{\mathbf{r}}_j = \mathbf{p}_j + \mathcal{U}_j, \quad d\theta_j = \left[\Omega_j + (\mathbf{p}_j \cdot \nabla)\mathcal{U}_j \cdot \mathbf{p}_j^{\perp}\right] dt + I_n dW.$$
 [1]

Here, $\mathbf{r}_j \equiv (x_j, y_j)$ and $\mathbf{p}_j \equiv (\cos \theta_j, \sin \theta_j)$ represent the position and heading direction of swimmer j. The vector \mathcal{U}_i denotes the fluid velocity created by all other swimmers at the location of swimmer j, Ω_i denotes a vision-based alignment and attraction response modulated by an anisotropic visual field modeling continuously a rear blind angle, and W(t) a standard Wiener process describing the spontaneous motion of the fish and modeling its "free will."

Emergent Collective Phases. We solved Eq. 1 numerically, starting from random initial conditions, to obtain the dynamical evolution of a school of N = 100 swimmers in a circular tank of radius R = 10. To analyze schools of comparable fish size and wall avoidance response, we fixed the values of $I_f=0.01$ and $I_w = 0.94$ (SI Appendix, Table S.1) and we varied the alignment I_a and noise I_n intensities (Fig. 1 and SI Appendix, Figs. S.2 and S.3 and Movies S.1-S.3). We observed the four characteristic phases of collective swimming: swarming, where swimmers form a disordered group with no preferential orientation; highly polarized schooling; milling, where all swimmers circulated in a vortex pattern in the same direction; and turning, where swimmers aligned along a preferential orientation while following a curved trajectory. The first three phases—swarming, schooling, and milling—have been observed in models with no hydrodynamic interactions or geometric confinement (6, 20). Turning emerges when hydrodynamic interactions are considered, independent of geometric confinement (21).

Under geometric confinement, the school exhibited two new phases not observed in unbounded domains: following the tank wall, where the school moved in the same direction, in a polarized manner that adhered to the tank wall, and double milling, where the swimmers split into two distinct subgroups, not necessarily of equal size, that milled in opposite directions, with individuals in each subgroup remaining in that subgroup, without switching direction. This double milling phase is topologically distinct from the elongated milling phase reported in ref. 20 in unbounded domains, where the swimmers organized themselves in two elongated, nearly parallel columns that crossed at both ends where swimmers did U-turns and reversed direction (SI Appendix, Fig. S.4).

In all ordered phases—schooling, milling, turning, and following the tank wall—flow interactions caused the average fish speed $\sum_{j=1}^{N} \|\dot{\mathbf{r}}_j\|/N$ to increase compared to solitary swimming, which we normalized to U = 1 in Eq. 1 (Movies S1–S3); this is consistent with the increase in speed noted in ref. 21. Importantly, in these states, the average speed also increased with increasing group size N (Movie S.4 and SI Appendix, Fig. S.6), thus recapitulating the experimental observations that average group speed positively correlates with local order (30) and school size (9). In our model, the increase in speed arises passively through hydrodynamics alone, without requiring active adjustment of the swimmer's speed in response to its perception of local order as proposed in ref. 9.

Statistical Order Parameters. To distinguish between these emergent collective phases, we used the global statistical order parameters P and $\Pi \in [0, 1]$,

$$P = \frac{1}{N} \left\| \sum_{j=1}^{N} \mathbf{p}_{j} \right\|, \qquad \Pi = \frac{1}{N} \left\| \sum_{j=1}^{N} \frac{(\mathbf{r}_{j} - \mathbf{r}_{c}) \times \dot{\mathbf{r}}_{j}}{\|\mathbf{r}_{j} - \mathbf{r}_{c}\| \|\dot{\mathbf{r}}_{j}\|} \right\|, \quad [2]$$

that represent, respectively, the degree of polarization and normalized angular momentum of the school relative to its center \mathbf{r}_c (SI Appendix, Fig. S.2). Highly polarized schools are characterized by P close to unity and Π close to zero. Milling

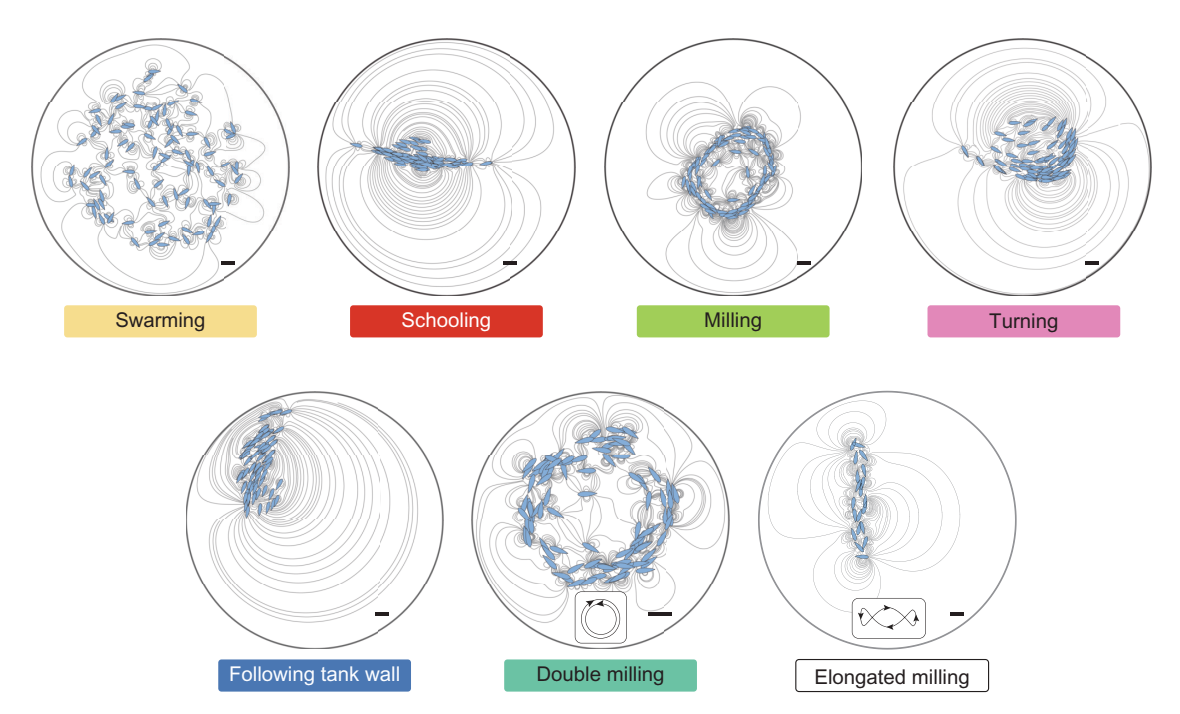


Fig. 1. Emergent collective phases in circularly confined swimmers. Swimmers are represented as airfoils of unit length to illustrate both their position and heading direction; scale bars correspond to unit length. Distinct dynamical phases emerge depending on parameter values: Swarming $I_a = 0.5$, $I_n = 0.9$; Schooling $I_a = 5$, $I_n = 0.6$; Milling $I_a = 1$, $I_n = 0.3$; Turning $I_a = 4$, $I_n = 0.1$; and Following the tank wall $I_a = 0.5$, $I_n = 0.15$. Double milling $I_a = 0.5$, $I_n = 0.1$. Elongated milling $I_a = 0.4$, $I_n = 0.1$, where swimmers organize in two columns that cross at both ends allowing swimmers to undergo U-turns. In all cases, $I_f = 0.01$, $I_f = 0.94$, and R = 10, except in double milling where R = 4 and R = 10, expect in elongated milling where R = 10, except in double milling where R = 10, except in double milling where R = 10, expect in elongated milling where R = 10, except in double milling where R = 10, except in elongated milling where R = 10, except in double milling where R = 10, except in elongated milling where R = 10, except in double milling where R = 10, except in elongated milling where R = 10, except in elongated milling where R = 10, except in double milling where R = 10, except in elongated milling elongated millin

motions have Π close to unity and low values of P. The swarming phase is characterized by both P and Π close to zero, and the turning phase by intermediate to high values of both P and Π . These observations are consistent with (21); we thus used the same threshold values of P and Π used in ref. 21 to characterize these four phases (*SI Appendix*, Algorithm S.1).

However, P and Π cannot distinguish between schooling and following the tank wall, both have values of P close to unity and low values of Π , nor between swarming and double milling, both have low values of P and Π . To resolve this ambiguity, we introduced two additional order parameters P_{wall} and $\Pi_{\text{mill}} \in [0,1]$ (SI Appendix, Figs. S.3 and S.4). The order parameter $P_{\text{wall}} = \left| \sum_{j=1}^{N} \mathbf{p}_j \cdot \mathbf{t}_j \right| / N$ measures the degree of agreement between the swimmer's heading \mathbf{p}_j and the local tangent \mathbf{t}_j to the wall. The order parameter $\Pi_{\text{mill}} = \sum_{j=1}^{N} \left\| (\mathbf{r}_j - \mathbf{r}_c) \times \dot{\mathbf{r}}_j \right\| / N \|\mathbf{r}_j - \mathbf{r}_c\| \|\dot{\mathbf{r}}_j\|$ measures the average magnitude of the angular momenta of individual swimmers; in contrast to Π , which is nearly zero when double milling, Π_{mill} is close to unity. In elongated milling, Π and Π_{mill} are both nearly zero (SI Appendix, Fig. S.4).

Bistable and Intermittent Collective Behavior. In addition to the two new phases—following the tank wall and double milling—the confined school exhibited bistable global modes of two distinct flavors: Depending on initial conditions but same parameter values, the school reached either schooling or milling and maintained it for the entire duration of the simulation (Fig. 2A); or, for the same initial conditions and parameter values, the school alternated at apparently random times between schooling and milling (Fig. 2B). While both behaviors indicate bistability, the latter is intermittent bistability or simply intermittency (Movie S.5).

The distinction between bistability and intermittent bistability is reflected in the time evolution of P and Π and is ensured only during the time integration period. In the bistable case, P remained consistently small and Π consistently near unity for all time when milling, and vice versa when schooling (Fig. 2C). In the intermittent case, P and Π dynamically switched from nearly zero to nearly unity as the school randomly alternated between schooling and milling. These dynamic transitions arise from random fluctuations in the directions of individuals imposed by the white noise in Eq. $\mathbf{1}$.

Confinement drove the switching between schooling and milling, as demonstrated through three types of parameter manipulations: increasing group size N (SI Appendix, Fig. S.7), aversion to boundary I_w (SI Appendix, Fig. S.8), and domain size R (SI Appendix, Fig. S.9). The switching rate decreased with increased school size (SI Appendix, Fig. S.7), consistent with experimental observations (9). It also decreased with increasing intensity of response to domain wall I_w and with increasing domain size R. That is, stronger interactions with boundaries resulted in higher switching rates. Meanwhile, changing the shape from circular to square domain had little effect on the switching rate (SI Appendix, Fig. S.10).

Histograms of Order Parameters and Dimensionality Reduction. We used Monte Carlo simulations with 100 realizations for each of the bistable and intermittent states and, in each simulation, discounted the first 20% of the total simulation time period T=1,000 to get rid of transient dynamics and form a multivariate histogram over the (P,Π) space (Fig. 2D and SI Appendix, Fig. S.5). This normalized histogram is a proxy for the steady-state probability density function (p.d.f.) of obtaining a collective pattern characterized by P and Π . The steady-state p.d.f.s of the bistable and intermittent behaviors are

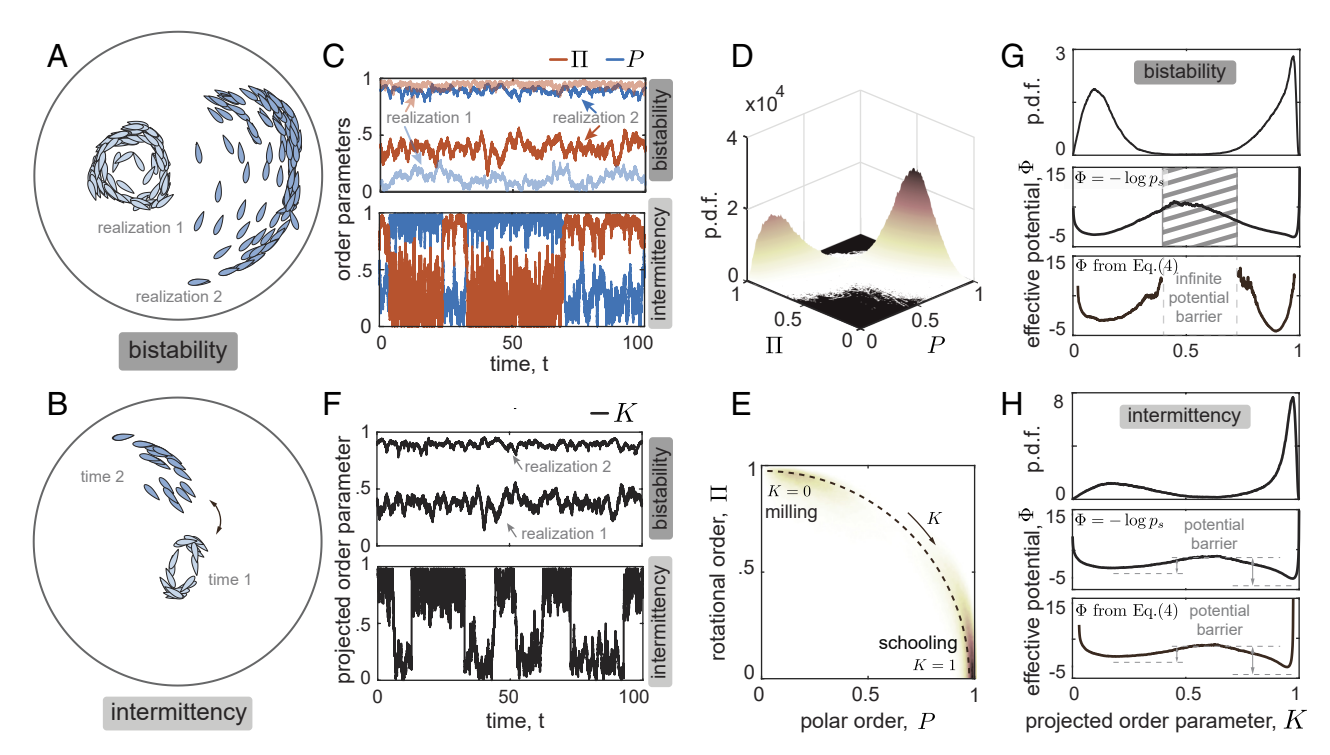


Fig. 2. Bistability and intermittency in the emergent collective behavior. (*A*) Bistable behavior for $I_a = 3$, $I_n = 0.1$. Depending on initial conditions, the swimmers self-organize in either a schooling or milling collective motion and maintain it for the entire duration of the simulation. (*B*) Intermittent bistability for $I_a = 3$, $I_n = 0.5$, where the group alternates between schooling and milling at random times, see Movie S.5. Switching rate depends on the school size (*SI Appendix*, Fig. S.7). (*C*) Time evolution of *P* and Π distinguishes between the bistable and intermittent behaviors. (*D*) Bimodal probability distribution function (p.d.f.) of polar and rotational order parameters *P* and Π based on Monte Carlo simulations with 100 trials for the parameter values in (*A*). Similar bimodal p.d.f. (not shown) is obtained for the parameter values in (*B*). (*E*) Projection of the p.d.f. onto the (*P*, Π) space shows that *P* and Π are correlated and occupy nearly a one-dimensional curved subspace of the (*P*, Π) space. A nonlinear principal component kernel is used to project *P* and Π onto this lower dimensional subspace, giving rise to a single projected order parameter *K*. (*F*) Time evolution of *K* distinguishes between the bistable and intermittent behaviors. (*G*) Bistable and (*H*) intermittent bimodal p.d.f.'s of the projected order parameters *K* and effective potentials $\Phi(K)$ constructed using $\Phi(K) = -\log(p_S(K))$ and from Eq. **4**. The former shows no distinction between bistability and intermittent bistability. This ambiguity is structural in the construction of $P_S(K)$ from data. Instead, Φ should be computed from Eq. **4**, where V(K) and D(K) are based on time-series data of the order parameter K(t).

nearly indistinguishable; we thus show only one in Fig. 2D. Both p.d.f.s are bimodal, with two peaks located at P near unity, corresponding to the schooling phase, and Π near unity, corresponding to the milling phase. But they represent different dynamics. In the bistable case, we observed no crossing from one peak to the other. The bimodal distribution arises from the superposition of two unimodel distributions with long tails, corresponding to either schooling or milling. In the intermittent case, the dynamics switched back and forth between the two peaks. Bimodality is inherent to the time evolution of the group.

A closer examination of the group dynamics showed that the domain of the bimodal p.d.f. is mostly confined to a nonlinear subspace of the (P,Π) plane (Fig. 2E). We thus used a nonlinear principal component analysis to identify and remove the nonlinear correlations between (P,Π) , reducing the dimensionality of (P,Π) to a one-dimensional subspace where the dynamics resides. We parameterized this subspace by K, where K=0 corresponds to milling and K=1 to schooling. Projecting the time evolution of P and Π onto the K-subspace preserves the dynamic characteristics of the bistable and intermittent behaviors (Fig. 2F): In the bistable case where distinct steady states are reached depending on initial conditions, K remained near unity at all time when schooling and near zero at all time when milling; in the intermittent case, K alternated dynamically between zero and one.

Phase Diagrams. To assess the relative importance of geometric confinement on the emergent collective phases, and transitions

among them, we performed a systematic parametric study over the phase space (I_n, I_a) in three limits of the model in Eq. 1 (Fig. 3 and *SI Appendix*, Fig. S.11): swimmers with vision-based and flow interactions in unbounded domain (21); circularly confined swimmers with vision-based but no flow interactions; and circularly confined swimmers with vision-based and flow interactions. To identify the emergent collective phase at each point (I_n, I_a) of the phase space, we run Monte-Carlo simulations with 100 realizations at each (I_n, I_a) , constructed the associated steady-state p.d.f.s of P, Π , P_{wall} and Π_{mill} by discarding the transient dynamics, and employed the classification *SI Appendix*, Algorithm S.1 to differentiate each of the emergent states reported in Figs. 1 and 2.

In unconfined domains, we recovered the results of ref. 21 for N=100 swimmers (Fig. 3A) with the four phases—swarming, milling, schooling, and turning—all appearing in the same regions of the phase space (I_n, I_a) as in ref. 21. In circularly confined domains with no flow interactions, the turning phase faded (Fig. 3B and SIAppendix, Fig. S.11), asserting that this phase relies on hydrodynamic interactions (21). Fish followed the tank wall in a significant region in the (I_n, I_a) space. Interestingly, confinement alone was sufficient to induce bistability and intermittent bistability. When the full model with flow interactions was considered (Fig. 3C), the two bistable phases persisted and the turning phase reappeared.

At smaller school size N=10, the collective phases shifted in the phase space and only intermittent bistability was observed (Fig. 3D). Direct comparison of the phase spaces at N=100

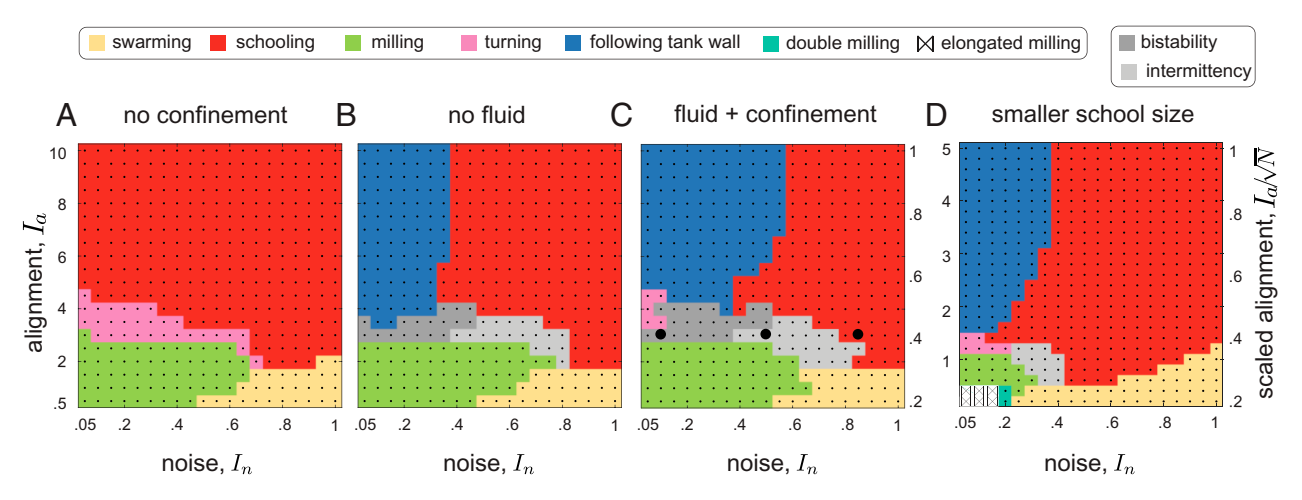


Fig. 3. Phase diagrams over the phase space (I_n , I_a): (A) Full model accounting for vision-based and hydrodynamic interactions in unbounded domain. (B) Vision-based model without hydrodynamic interactions in geometric confinement. (C) Full model accounting for vision-based and hydrodynamic interactions in geometric confinement. Distinct collective patterns are represented by their unique color code based on the value of the order parameters P and Π . Classification at each point (I_n , I_a) is based on Monte-Carlo simulations of 100 trials and *SI Appendix*, Algorithm S.1. In all simulations, $I_f = 10^{-2}$, $I_W = 0.94$, R = 10, N = 100 in panels (A–C), and N = 10 in panel (D).

and N=10 shows that the group size affects the emergent phases in a nontrivial manner beyond what can be explained by a mere rescaling of parameters. At N=10, double milling and elongated milling appeared at low noise and alignment intensities. To probe the mechanisms leading to these phases, we repeated the computations for N=10 in the unbounded domain with flow interactions and in circular confinement without flow interactions (*SI Appendix*, Fig. S.11). We found that elongated milling appeared under no confinement, consistent with (20), but double milling required confinement, emphasizing the distinction between these two phases and that double milling is a confinement-induced collective phase.

To examine how school density $\rho = N/\pi R^2$ affected emergent behavior, we fixed the parameter values (I_n, I_a) and varied R and N independently. In Fig. 4A, we observed a transition from milling to intermittent milling-schooling that seemed to depend only on ρ . However, in Fig. 4B, transitions from milling to double milling and from milling to elongated milling occurred at the same density levels. In Fig. 4C, we show the histograms of statistical order parameters corresponding to two schools of fish at the same density value; the results recapitulate experimental observations (9, Fig. 2): The larger school in the larger domain exhibited high rotational order, characteristic of the milling state, while the smaller school in the smaller domain, despite having the same density, displayed low polarization and rotational order. These findings indicate that, in the presence of boundaries, the collective states depend explicitly on the number of fish N and tank size R, not only through their influence on the group density $\rho = N/\pi R^2$, because of the nontrivial interplay of boundary interactions and individual level noise.

Probabilistic Description of Collective Dynamics. To characterize the collective dynamics, we applied a general probabilistic approach considering the probability density function $p(P, \Pi, t)$ is governed by a Fokker–Planck equation (31). Because we are interested in the bistable states where the dynamics lies on a one-dimensional subspace of the (P, Π) space (Fig. 2), we set out to describe the group dynamics in terms of the single coarsegrained order parameter K(t) and associated probability density function p(K, t). Starting from the assumption that the time evolution of K is governed by an Itô stochastic differential

equation $dK = V(K)dt + \sqrt{2D(K)}dW$, with white Gaussian noise (which we justify a posteriori), it follows immediately that the time evolution of p(K, t) is governed by an effective Fokker–Planck equation (32)

$$\frac{\partial p(K,t)}{\partial t} = -\frac{\partial}{\partial K} \left[V(K) p(K,t) \right] + \frac{\partial^2}{\partial K^2} \left[D(K) p(K,t) \right], \quad [3]$$

where the drift V(K) and diffusion D(K) > 0 coefficients (both scalars) are related, respectively, to the time evolution of the first two moments of K(t) (SI Appendix, section S.4). The solution to the steady-state Fokker–Planck equation $(\partial p/\partial t = 0)$ is a stationary probability density function $p_s(K)$ that defines an effective potential $\Phi(K)$ such that $p_s(K) \sim \exp(-\Phi(K))$. The effective potential $\Phi(K)$ also satisfies

$$\Phi(K) = \log(D(K)) - \int_{-\infty}^{K} \frac{V(K')}{D(K')} dK' + \text{constant.}$$
 [4]

Effective Potential of Stationary Probability Density Function.

We constructed the stationary p.d.f. $p_s(K)$ from Monte Carlo simulations for the bistable and intermittent states of Fig. 2. In Fig. 2 G and H, we show $p_s(K)$ and the corresponding $\Phi(K)$ constructed using $\Phi(K) = -\log(p_s(K))$. Additionally, we constructed the effective potential $\Phi(K)$ from Eq. 4 by estimating V(K) and D(K) using ensembles of long-time simulations (22, 24) (SI Appendix, section S.4).

In the bistable state, the effective potential Φ estimated from Eq. 4 is characterized by an infinite potential barrier between the two wells corresponding to stable milling and stable schooling (Fig. 2G). This is consistent with the corresponding collective dynamics in Fig. 2A, where the school reached, depending on initial conditions, one of these states but did not cross between them. The effective potential $\Phi(K)$ calculated from $p_s(K)$ missed this important feature, erroneously predicting a finite potential barrier between the two states. This error is inherent to constructing a single steady-state distribution $p_s(K)$ that can, in principle, converge to either state. If initial conditions were within the basin of attraction of one of the two states, the result would be a unimodal steady-state distribution with a long tail. However, because initial conditions are randomly sampled from

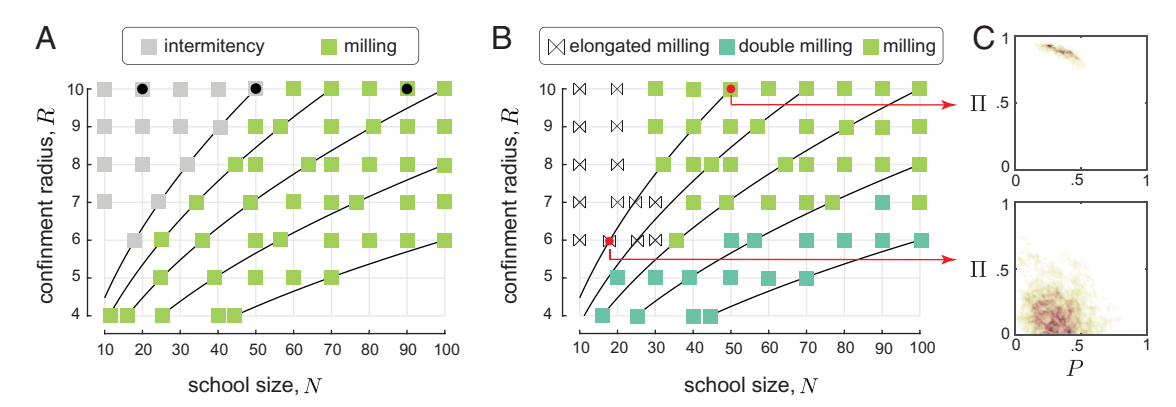


Fig. 4. Phase diagrams over the space (N, R) for swimmers following vision-based rules and flow interactions in geometric confinement. Solid lines indicate constant number density $N/\pi R^2$. (A) $I_a = 0.8$, $I_n = 0.3$. (B) $I_a = 0.4$, $I_n = 0.1$. In all simulations, $I_f = 10^{-2}$ and $I_W = 0.94$. (C) P.d.f.'s of polar and rotational order parameters P and Π for distinct values of N and R but same density ($\rho = N/\pi R^2 = \text{constant}$) exhibit different emergent phases: milling at larger N and R and elongated milling (lower P and Π) at proportionally smaller N and R.

both basins of attraction, the outcome is a bimodal steady-state distribution $p_s(K)$ with connected peaks. But this connection is not dynamic. In the intermittent state, the effective potential Φ estimated from Eq. 4 and that calculated directly from $p_s(K)$ exhibited a finite potential barrier between the two states that can be overcome by white noise (Fig. 2*H*). Therefore, evaluating Φ directly from steady-state distribution of $p_s(K)$ is structurally ambiguous in that it does not distinguish between bistability and intermittent bistability; instead, Φ should be evaluated dynamically using Eq. 4, where V(K) and D(K) are based on time-series data of the order parameter K(t).

Bifurcations in the Collective Dynamics. We next used the coarse-grained dynamics to analyze the transitions highlighted by black markers "•" in Figs. 3C and 4A. At each of these parameter values, we constructed the corresponding bivariate p.d.f.s on the (P,Π) space (colormap, *Left*) and computed the effective potential $\Phi(K)$ on the reduced K-space (black lines, Right); see Fig. 5 A and C. Values of K at the local minima of $\Phi(K)$ and the corresponding probability flux $\partial \Phi / \partial K$ are superimposed onto the p.d.f.s in the (P, Π) space (Left). The excellent agreement between data and $\partial \Phi / \partial K$ verifies a posteriori the validity of the built-in assumption in the Fokker-Planck description that the time evolution of K follows a stochastic differential equation with additive white noise.

Fig. 5A analyzes the transition from bistable schooling and milling to monostable schooling with increasing I_n . At small I_n , the effective potential has two potential wells separated by an infinite potential barrier, reflecting either schooling or milling but no transition between the two phases. As noise increased, the infinite barrier became finite, leading to a double-well potential Φ with finite potential barrier surmountable by noise at the individual swimmer level. This reflects a transition to intermittency between schooling and milling. As noise increased further, the potential well corresponding to stable milling disappeared leaving only one potential well for schooling. This is counterintuitive because, while noise is necessary to transition between milling and schooling, too much noise completely destroys the milling state, leaving only one potential well corresponding to schooling.

Borrowing tools from deterministic bifurcation theory (22), we followed the critical points of the effective potential as I_n increased (Fig. 5B). Values of K corresponding to local minima of Φ indicate points on the stable branch of the bifurcation diagram, and values of K corresponding to local maxima of Φ indicate points on the unstable branch. In determining the maxima, we performed a quadratic fit of the effective potential between the two prominent wells to filter out spurious highfrequency numerical errors. The bifurcation diagram in Fig. 5B indicates that the transition from bistable to intermittent behavior is a smooth cross-over, whereas the transition from intermittency to schooling is a sudden phase transition typical of a saddle-node bifurcation at $I_n = 0.75$.

Additionally, we calculated the fraction of residence time T_{milling}/T in the milling state (Fig. 5*B*). By definition, the escape rate from the milling state is equal to $1 - T_{\text{milling}}/T$. We found that, in the bistable regime, the escape rate is either zero (when milling is stable) or one (when schooling is stable), while in the intermittent regime, the residence time decays quasi-linearly with increasing noise intensity I_n .

Fig. 5C analyzes the transition from bistable schooling and milling to monostable milling with increasing N. For a relatively small school of size N=20, the double-well potential Φ is characterized by a finite potential barrier surmountable by noise, reflecting that the group intermittency between schooling and milling. As N increased, the potential well corresponding to schooling became more shallow, and at even larger N, it suddenly disappeared altogether, leaving only stable milling. The corresponding bifurcation diagram in Fig. 5D indicates two transitions from monostable to bistable and back to monostable behavior as N increased from N = 2 to N = 100, both typical of abrupt phase transitions as those observed in saddle-node bifurcations. The residence time in the milling state increased quasi-linearly with larger school size, consistent with empirical observations (SI Appendix, Fig. S.7).

Discussion

We developed a mathematical model of fish schools that integrated geometric confinement into existing data-inferred behavioral rules (18) and flow interactions (21). We analyzed the model extensively, demonstrating the emergence of new collective patterns and spontaneous transitions between milling and schooling driven by geometric confinement and interactions with domain boundaries. These transitions and the mechanisms driving them are fundamentally different from transitions in unbounded domains through fine adjustments of alignment and attraction parameters (20) or through rare injection of large rotational noise (22).

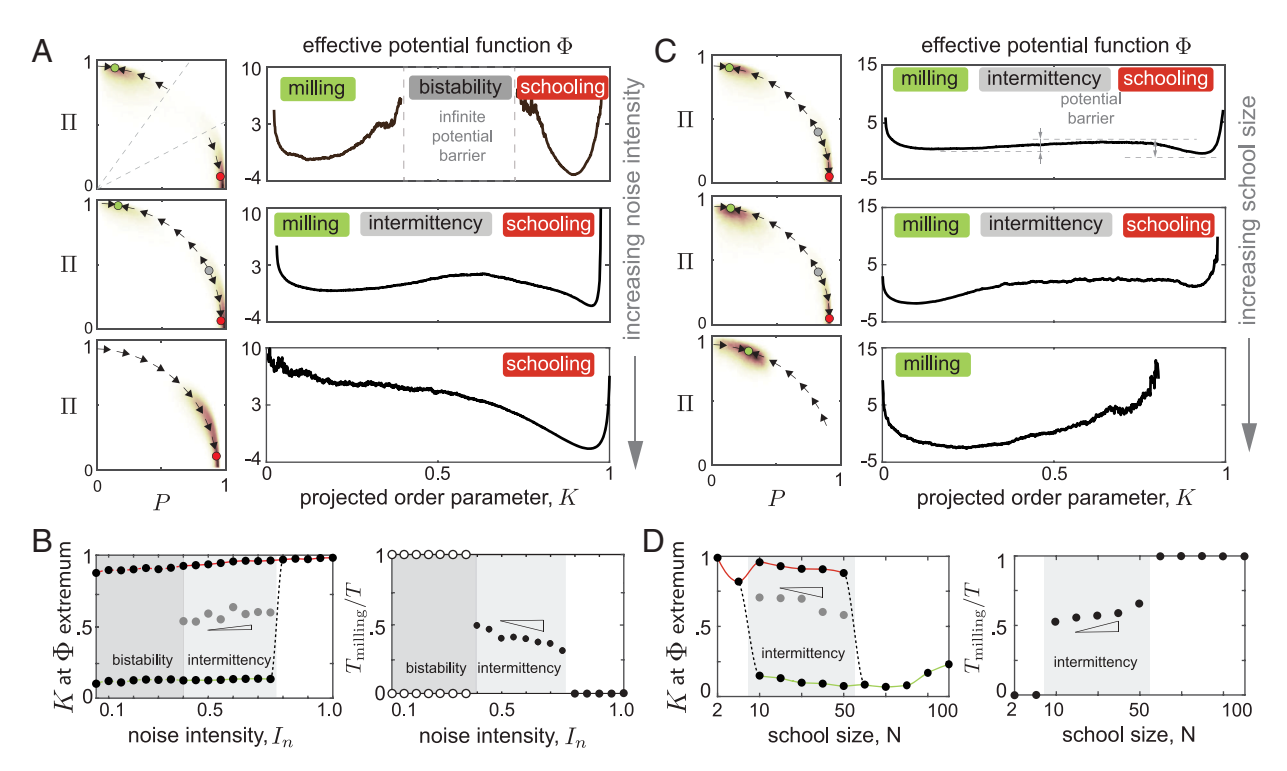


Fig. 5. Bifurcations and phase transitions in the emergent collective patterns. (*A*) P.d.fs of *P* and Π (*Left*) and corresponding effective potential (*Right*) for three distinct noise levels $I_n = 0.1, 0.5, 0.85$ and constant $I_a = 3$, corresponding to the black markers "•" in Fig. 3*C*. Probability flux $\partial \Phi / \partial K$ (black arrows) and *K*-values at the minima and maxima of Φ (round markers) are superimposed onto the p.d.f.'s of *P* and Π (*Left*). As I_n increases, the school transitions from bistable to intermittent and finally to schooling. (*B*) Bifurcation diagram of *K* versus I_n : stable (black markers)/unstable (gray markers) stationary solutions of the Fokker-Planck equations correspond to minima/maxima of Φ. The two stable branches transition smoothly from bistability to intermittent bistability. Stable milling disappears suddenly at $I_n = 0.75$, presumably by colliding with the unstable branch in a saddle-node bifurcation leading to only a single stable branch corresponding to schooling. Fraction of residence time in the milling state decays quasi-linearly in the intermittent regime with increasing noise. (*C*) P.d.f's of *P* and Π (*Left*) and corresponding effective potential for three distinct school size N = 20, 50, 90 and R = 10, corresponding to the black markers "•" in Fig. 4A. $\partial \Phi / \partial K$ (black arrows) and *K*-values at the minima and maxima of Φ (round markers) are superimposed onto the p.d.f.'s of *P* and Π (*Left*). As school size increases, the school transitions from intermittent behavior to milling. (*D*) Bifurcation diagram indicates the existence of two saddle-node bifurcations. Fraction of residence time in the milling state increases quasi-linearly in the intermittent regime with increasing school size.

A key feature of our work is that, instead of using smart but ad hoc manipulations of statistical order parameters to characterize the transitions between milling and schooling (9, 20, 22), we went beyond mere statistics to provide a probabilistic description of the time evolution of the group. Our two-step approach for mapping microscopic (individual) to macroscopic (group) dynamics first eliminated correlations between statistical order parameters through a nonlinear projection onto a onedimensional subspace with a single coarse-grained variable; then, inspired by refs. 22 and 24, we formulated a Fokker-Planck equation and constructed effective potential landscapes that governed the emergent collective states (Figs. 2 and 5). Confinement-driven dynamic transitions between milling and schooling corresponded to a double-well potential with bistable states separated by a finite potential barrier (Fig. 5), allowing transitions to be triggered entirely by individual-level noise with no change in individual rules or parameters. Double-well potentials with infinite potential barrier led to either stable milling or stable schooling but no dynamic switching between the two, at least not during the time period of the numerical integration. These two flavors of bistability are indistinguishable by a mere examination of p.d.f.s of the coarse-grained variables (Fig. 2). The distinction is dynamic. Constructing effective potentials from time evolution data of the coarse-grained variable was thus essential for the classification of group dynamics and phase transitions and for uncovering that the transition from bistable to intermittent behavior is a smooth cross-over, while the

transition from bistable to monostable states is a phase transition where one stable state suddenly disappeared, likely following collision with an unstable state (Fig. 5).

Predictions from our model displayed notable parallels to empirical observations in groups of golden shiners (Notemigonus crysoleucas) confined in shallow water tanks (9), including correctly predicting the spontaneous switching between milling and schooling (9, Figs.1 and 2), with increased average speed and decreased rate of switching as group size increased and transition to only milling in larger groups (Figs. 2 and 5*C* and *SI Appendix*, Figs. S.6 and S.7). We also found that maintaining the same group density but proportionally decreasing the number of fish and tank size induced a transition from milling to swarming (Fig. 4*B*) consistent with experimental findings (9, Fig. 2). That is, in contrast to classic self-propelled particle models in unbounded or periodic domains (14), in the presence of confinement and interactions with external boundaries, group density alone does not control the collective behavior.

Our analysis provides insights and testable hypotheses into how geometric confinement affects collective patterns and triggers phase transitions between different collective states in schooling fish. The new collective patterns—following the domain wall and double milling—could offer functional advantages to the group. Schooling fish might stay near and move along boundaries because these areas are often nutrient-rich and offer a strategic advantage for detecting and evading potential threats. From a synchronization perspective, milling is akin to in-phase

synchronization of coupled oscillators, whereas double milling resembles antiphase synchronization (33). Double milling, while not documented in prior studies of schooling fish, appears to occur in groups of fish confined in shallow water and within tank boundaries, such as in fish farms. This behavior might help in mixing nutrients and oxygen more effectively within confined crowded groups (34).

In natural conditions, schools of fish inhabiting large enclosures might benefit from the ability to spontaneously switch between milling and schooling; in the milling phase, the school remains within a limited space while in the schooling phase, it explores a larger domain. Repeated switching between milling and schooling could provide a functional advantage by allowing a school of fish to regularly explore its environment, for surveillance or foraging, without incurring additional costs or requiring changes in sensing and behavior at the individual level. Yet, even a subtle adjustment in individual behavior, such as increased noise in response to environmental perturbations or increased group size, could enable the school to transition to a monostable state of schooling or milling through the sudden collapse of global stable states, potentially providing unique advantages such as evading or confusing predators.

Beyond fish schools, our work paves the way toward creating a general data-driven framework for understanding how environmental factors influence self-organization and collective

- 1. V. Magidson et al., The spatial arrangement of chromosomes during prometaphase facilitates spindle assembly. Cell 146, 555-567 (2011).
- C. Guillot, T. Lecuit, Mechanics of epithelial tissue homeostasis and morphogenesis. Science 340, 1185-1189 (2013).
- I. D. Couzin, J. Krause, N. R. Franks, S. A. Levin, Effective leadership and decision-making in animal groups on the move. Nature 433, 513-516 (2005).
- M. Ballerini et al., Interaction ruling animal collective behavior depends on topological rather than metric distance: Evidence from a field study. Proc. Natl. Acad. Sci. U.S.A. 105, 1232-1237 (2008).
- D. V. Radakov, Schooling in the Ecology of Fish (J. Wiley, 1973).
- I. D. Couzin, J. Krause, R. James, G. D. Ruxton, N. R. Franks, Collective memory and spatial sorting in animal groups. J. Theor. Biol. 218, 1-11 (2002).
- A. Berdahl, C. J. Torney, C. C. Ioannou, J. J. Faria, I. D. Couzin, Emergent sensing of complex environments by mobile animal groups. Science 339, 574-576 (2013).
- D. J. Sumpter, Collective Animal Behavior (Princeton University Press, 2010)
- K. Tunstrøm et al., Collective states, multistability and transitional behavior in schooling fish. PLoS Comput. Biol. 9, e1002915 (2013).
- 10. C. C. Ioannou, V. Guttal, I. D. Couzin, Predatory fish select for coordinated collective motion in virtual prey. Science 337, 1212-1215 (2012).
- 11. M. M. Sosna et al., Individual and collective encoding of risk in animal groups. Proc. Natl. Acad. Sci. U.S.A. 116, 20556-20561 (2019).
- 12. I. Aoki, A simulation study on the schooling mechanism in fish. Nippon Suisan Gakkaishi 48, 1081-1088 (1982)
- 13. A. Huth, C. Wissel, The simulation of the movement of fish schools. J. Theor. Biol. 156, 365-385 (1992).
- 14. T. Vicsek, A. Czirók, E. Ben-Jacob, I. Cohen, O. Shochet, Novel type of phase transition in a system of self-driven particles. Phys. Rev. Lett. 75, 1226 (1995).
- 15. G. Ódor, Universality classes in nonequilibrium lattice systems. Rev. Mod. Phys. 76, 663 (2004)
- 16. J. Toner, Y. Tu, S. Ramaswamy, Hydrodynamics and phases of flocks. Ann. Phys. 318, 170-244 (2005)
- 17. M. C. Marchetti et al., Hydrodynamics of soft active matter. Rev. Mod. Phys. 85, 1143-1189
- 18. J. Gautrais et al., Deciphering interactions in moving animal groups. PLoS Comput. Biol. 8, e1002678 (2012).
- 19. D. S. Calovi et al., Disentangling and modeling interactions in fish with burst-and-coast swimming reveal distinct alignment and attraction behaviors. PLoS Comput. Biol. 14, e1005933 (2018).
- 20. D. S. Calovi et al., Swarming, schooling, milling: Phase diagram of a data-driven fish school model. N. J. Phys. 16, 015026 (2014).

dynamics and for designing control strategies that induce or suppress phase transitions in out-of-equilibrium active systems by tuning environmental parameters, such as geometric confinement (28, 35, 36), intensity or pattern of illumination (23, 37), and electric field intensity (38).

Materials and Methods

Fish in circular confinement are modeled as self-propelled dipolar particles following vision-based behavioral rules and interacting with domain boundaries. Mapping from individual to group dynamics obeys a Fokker-Planck equation, where the drift and diffusion coefficients are constructed directly from timeevolution of the coarse-grained variables. Detailed derivation of equations of motion, both at the individual and collective levels, can be found in SI Appendix, together with eleven supporting figures.

Data, Materials, and Software Availability. All study data are included in the article and/or supporting information. Data have been deposited to Github (39).

ACKNOWLEDGMENTS. Funding provided by the National Science Foundation grants Research Advanced by Interdisciplinary Science and Engineering IOS-2034043 and CBET-210020 and the Office of Naval Research grants N00014-22-1-2655 and N00014-19-1-2035 (all to E.K.).

- 21. A. Filella, F. Nadal, C. Sire, E. Kanso, C. Eloy, Model of collective fish behavior with hydrodynamic interactions. Phys. Rev. Lett. 120, 198101 (2018).
- $22. \quad A.\ Kolpas,\ J.\ Moehlis,\ I.\ G.\ Kevrekidis,\ Coarse-grained\ analysis\ of\ stochasticity-induced\ switching$ between collective motion states. Proc. Natl. Acad. Sci. U.S.A. 104, 5931-5935 (2007).
- 23. B. Lafoux, J. Moscatelli, R. Godoy-Diana, B. Thiria, Illuminance-tuned collective motion in fish. Commun. Biol. 6, 585 (2023).
- J. Gradišek, S. Siegert, R. Friedrich, I. Grabec, Analysis of time series from stochastic processes. Phys. Rev. E 62, 3146 (2000).
- A. C. H. Tsang, E. Kanso, Dipole interactions in doubly periodic domains. J. of Nonlinear Sci. 23, 971-991 (2013).
- 26. A. A. Tchieu, E. Kanso, P. K. Newton, The finite-dipole dynamical system. Proc. R. Soc. A Math. Phys. Eng. Sci. 468, 3006-3026 (2012).
- 27. E. Kanso, A. C. H. Tsang, Dipole models of self-propelled bodies. Fluid Dyn. Res. 46, 061407
- 28. A. C. H. Tsang, E. Kanso, Circularly confined microswimmers exhibit multiple global patterns. Phys. Rev. E 91, 043008 (2015).
- 29. L. M. Milne-Thomson, Theoretical Hydrodynamics (Dover Publications, ed. 5, 2011).
- 30. S. V. Viscido, J. K. Parrish, D. Grünbaum, Individual behavior and emergent properties of fish schools: A comparison of observation and theory. Mar. Ecol. Prog. Ser. 273, 239-249 (2004).
- 31. D. T. Gillespie, The multivariate langevin and fokker-planck equations. Am. J. Phys. 64, 1246-1257 (1996).
- 32. R. Jordan, D. Kinderlehrer, F. Otto, The variational formulation of the fokker-planck equation. SIAM J. Math. Anal. 29, 1-17 (1998).
- 33. S. H. Strogatz, I. Stewart, Coupled oscillators and biological synchronization. Sci. Am. 269, 102-109 (1993).
- 34. B. G. Oskouei, E. Kanso, P. K. Newton, Streamline bifurcations and scaling theory for a multiplewake model. Int. J. Non-Linear Mech. 46, 592-601 (2011).
- 35. E. Lushi, H. Wioland, R. E. Goldstein, Fluid flows created by swimming bacteria drive selforganization in confined suspensions. Proc. Natl. Acad. Sci. U.S.A. 111, 9733-9738 (2014).
- 36. A. C. H. Tsang, E. Kanso, Density shock waves in confined microswimmers. Phys. Rev. Lett. 116, 048101 (2016).
- 37. Z. Zarei et al., Light-activated microtubule-based two-dimensional active nematic. Soft Matter 19, 6691-6699 (2023).
- J. Yan et al., Reconfiguring active particles by electrostatic imbalance. Nat. Mater. 15, 1095-1099
- 39. C. Huang, F. Ling, E. Kanso, Collective phase transitions in confined fish schools. Github. https:// github.com/ekanso/Collectivephasetransitionsinconfinedfishschools. Deposited 14 October 2024.